고차전단변형을 고려한 적층복합판 및 쉘의 열-습윤 휨해석

Hygrothermal Bending Analysis of Laminated Composite Plates and Shells Considering a Higher-order Shear Deformation

한 성 천* 윤 석 호**
Han, Sung-Cheon Yoon, Seok-Ho

요 지

비등방성으로 적층된 복합판 및 쉘구조물에서 온도와 습도의 급격한 변화는 구조물의 강도와 성능을 저하시키는 중요한 원인이 된다. 더욱이 하중에 의한 역학적 변위와 조합될 때에는 좌굴, 대변형 혹은 고응력 상태를 유발하게된다. 본 연구에서는 이중 퓨리에급수를 이용하여 3차의 전단변형함수로 가정된 평형방정식을 전개하고 폭-두께비, 형상비의 변화 그리고 재료의 성질에 따른 결과에 대하여 고찰하였다.

핵심용어 : 복합적층판 및 쉘, 열-습윤효과, 폭-두께비, 형상비, 고차전단변형

Abstract

The presence of elevated temperature and moisture can alter significantly the structural response of laminated composite plates and shells. A hygrothermal environment causes degradation in both strength and constitutive properties, particularly in the case of fibre-reinforced polymeric structures. Futhermore, associated hygrothermal expansion, either alone or in combination with mechanically induced deformation, can result in buckling, large deflections, and excessively high stress levels. Consequently, it is often imperative to consider environmental effects in the analysis and design of anisotropic systems. This paper focuses on hygrothermally induced deformation behaviour of anisotropic structures and expand the third-order shear deformation theory by the Double-Fourier series. Numerical results for deflections are presented showing the effect of side-to-thickness ratio, aspect ratio, material anisotropy.

Keywords : *laminated composite plates and shells, hygrothermal effects, side-to-thickness ratio, aspect ratio, higher-order shear deformation*

1. INTRODUCTION

With the increased use of fiber-reinforced composites in civil, aerospace and mechanical engineering structures, studies involving the thermomechanical behavior of composite ma-

* 정회원·대원공과대학 토목과, 조교수
** 정회원·경동대학교 토목설계공학과, 전임강사

• 이 논문에 대한 토론을 1999년 6월 30일까지 본 학회에 보내주시면 1999년 9월호에 그 결과를 게재하겠습니다.

terial plates and shells are receiving greater attention. Most of the previous research in the field of composites deals with isothermal problems. However, use of composites in environments with large temperature change (e.g., in applications such as the space shuttle) requires the knowledge of hygrothermally induced deflection and stresses. Recent studies in analysis of plates and shells that are laminates of fiber-reinforced materials indicate that the thickness effect (i.e., shear deformation) on behavior of the plates and shells is more pronounce than in isotropic plates and shells.

The problem of thermal bending of anisotropic plates was first studied by Pell[1], who derived the equations governing the transverse deflection of a thin plate. Whintney and Ashton[2] studied the effects of moisture on the elastic response of layered composite plates. The shear deformation theory that has been proved to be adequate in predicting the overall response of laminated anisotropic plates is that of Whitney[3].

The present investigation is concern with the application of analytical method using double-Fourier series and higher-order shear deformation theory to hygrothermal effects of layered anisotropic composite plates and shells.

Our models are presented for equations governing simply supported, rectangular, antisymmetric angle-ply, cross-ply plates and shells under sinusoidal hygrothermal loadings on multi-layers laminated plates and shells of a fiber-reinforced material.

Numerical results for deflections are presented showing the effect of side-to-thickness ratio, material anisotropy and comparing with first-order shear deformation theory and classical theory.

2. GOVERNING EQUATIONS

Consider a laminated shallow shell composed of N orthotorpic laimnates.

Fig. 1(a) contains a differential element of a doubly curved shell. Here (ξ_1, ξ_2, ζ) denote the orthogonal curvilinear coordinates (or shell coordinates) such that ξ_1 and ξ_2 curves are lines of principle curvature on midsurface $\zeta=0$, and ζ curves (also refered to as z) are straight lines perpendicular to the midsurface. The raddi of cuvatures along the ξ_1 and ξ_2 curves are R_1 and R_2, respectively. The reference surface Ω coincides with the midsurface. The position vector of a point on the midsurface is denoted by $\underline{r}$, and the position vector of a point at distance ζ from the midsurface is denoted by $\underline{R}$ [see Fig. 1(b)].

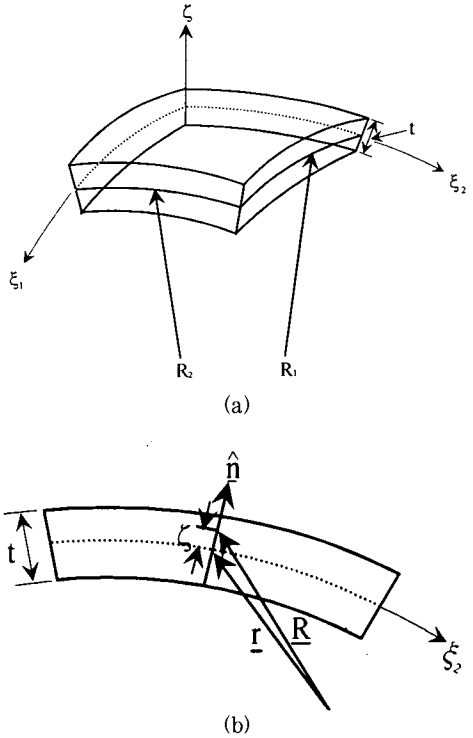

Fig. 1 Geometry of doubly curved shell

The distance ds between two points on the midsurface is determined by

$$(ds)^2=d\underline{r}\cdot d\underline{r}=\alpha_1^2(d\xi_1)^2+\alpha_2^2(d\xi_2)^2 \quad (1)$$

where α_1^2 and α_2^2 are the midsurface metrices. The distance dS between pointsrm (ξ_1, ξ_2, ζ) and $(\xi_1+d\xi_1, \xi_2+d\xi_2, \zeta+d\zeta)$ is given by

$$(dS)^2=d\underline{R}\cdot d\underline{R}=L_1^2(d\xi_1)^2 +L_2^2(d\xi_2)^2+L_3^2(d\zeta)^2 \quad (2)$$

where L_1, L_2 and L_3 are the Lam′e coefficients

$$L_1=\alpha_1\left(1+\frac{\zeta}{R_1}\right),\ L_2=\alpha_2\left(1+\frac{\zeta}{R_2}\right),\ L_3=1 \quad (3)$$

Following the procedure similar to that presented in [3] for flat plates, we begin with the following displacement field

$$\begin{aligned}\bar{u}(\xi_1,\ \xi_2,\ \zeta)&=\frac{1}{\alpha_1}L_1u+\zeta\phi_1+\zeta^2\psi_1+\zeta^3\theta_1\\ \bar{v}(\xi_1,\ \xi_2,\ \zeta)&=\frac{1}{\alpha_2}L_2v+\zeta\phi_2+\zeta^2\psi_1+\zeta^3\theta_1\\ \bar{w}(\xi_1,\ \xi_2,\ \zeta)&=w\end{aligned} \quad (4)$$

Substitutimg Eq. (3) for Eq. (4), one obtains

$$\begin{aligned}\bar{u}(\xi_1,\ \xi_2,\ \zeta)&=\left(1+\frac{\zeta}{R_1}\right)u+\zeta\phi_1+\zeta^2\psi_1+\zeta^3\theta_1\\ \bar{v}(\xi_1,\ \xi_2,\ \zeta)&=\left(1+\frac{\zeta}{R_2}\right)v+\zeta\phi_2+\zeta^2\psi_1+\zeta^3\theta_1\\ \bar{w}(\xi_1,\ \xi_2,\ \zeta)&=w\end{aligned} \quad (5)$$

where $(\bar{u}, \bar{v}, \bar{w})$ are the displacement (u, v, w) coordinates, are the displacement of a point on the middle surface and ϕ_1 and ϕ_2 are the rotation at $\zeta=0$ of normals to the midsurface with respect to the ξ_1 and ξ_2 axes, respectively. The particular choice of the displacemet field in Eq. (5) is dictated by the desire to represent the transverse shear strains by quadratic functions of the thickness coordinate, ζ, and by the requirement that the transverse normal strain be zero.

The functionrm ψ_i and θ_i will be determined using the condition that the transverse shear stresses vanish on the top and bottom surfaces of the shell. Substituting ψ_i and θ_i for Eq. (5), one obtains

$$\begin{aligned}\bar{u}(\xi_1\ \xi_2,\ \zeta)&=\left(1+\frac{\zeta}{R_1}\right)u+\zeta\phi_1 +\zeta^3\left(\frac{4}{3t^2}\right)\left[-\phi_1-\frac{1}{\alpha_1}\frac{\partial w}{\partial\xi_1}\right]\\ \bar{v}(\xi_1,\ \xi_2,\ \zeta)&=\left(1+\frac{\zeta}{R_2}\right)v+\zeta\phi_2 +\zeta^3\left(\frac{4}{3t^2}\right)\left[-\phi_2-\frac{1}{\alpha_2}\frac{\partial w}{\partial\xi_2}\right]\\ \bar{w}(\xi_1,\ \xi_2,\ \zeta)&=w\end{aligned} \quad (6)$$

The constitutive relations with hygrothermal effects, for a typical layer k of a laminate using the Cartesian coordinates $(dx_i=\alpha_i d\xi,\ i=1, 2)$, can be written as[4), 5)]

$$\begin{Bmatrix}\sigma_x\\ \sigma_y\\ \sigma_{xy}\end{Bmatrix}=\begin{bmatrix}\bar{Q}_{11}&\bar{Q}_{12}&\bar{Q}_{16}\\ \bar{Q}_{12}&\bar{Q}_{22}&\bar{Q}_{26}\\ \bar{Q}_{16}&\bar{Q}_{26}&\bar{Q}_{66}\end{bmatrix}\begin{Bmatrix}\varepsilon_x-\bar{\alpha}_1\Delta T-\bar{\beta}_1\Delta M\\ \varepsilon_y-\bar{\alpha}_2\Delta T-\bar{\beta}_2\Delta M\\ \varepsilon_{xy}-\bar{\alpha}_6\Delta T-\bar{\beta}_6\Delta M\end{Bmatrix}$$

$$\begin{Bmatrix}\sigma_{xz}\\ \sigma_{yz}\end{Bmatrix}=\begin{bmatrix}\bar{Q}_{55}&\bar{Q}_{45}\\ \bar{Q}_{45}&\bar{Q}_{44}\end{bmatrix}\begin{Bmatrix}\varepsilon_{xz}\\ \varepsilon_{yz}\end{Bmatrix} \quad (7)$$

in which $\bar{Q}_{ij}$ and $\bar{\alpha}_i$, $\bar{\beta}_i$ denote the transformed material coefficients. ΔT, ΔM denotes temperature and moisture rise in the laminates and is given by[6)]

$$\Delta T=T_0+zT_1,\ \Delta M=M_0+zM_1 \quad (8)$$

The equilibrium equation of the theory can be obtained from the total potential energy principle

$$\delta \Pi = 0$$

where Π is the total potential energy,

$$\Pi = \frac{1}{2}\int_V [\sigma_x\varepsilon_x + \sigma_y\varepsilon_y + \sigma_{yz}\varepsilon_{yz} + \sigma_{xz}\varepsilon_{xz} + \sigma_{xy}\varepsilon_{xy}]dxdydz - \int_R qwdxdy \tag{9}$$

Therefore, the application of the principle of total potential energy gives the following five equations;[7]

$$\frac{\partial N_1}{\partial x} + \frac{\partial N_6}{\partial y} - \frac{\partial}{\partial x}(N_1^T + N_1^M) - \frac{\partial}{\partial y}(N_6^T + N_6^M) = 0$$

$$\frac{\partial N_6}{\partial x} + \frac{\partial N_2}{\partial y} - \frac{\partial}{\partial y}(N_2^T + N_2^M) - \frac{\partial}{\partial x}(N_6^T + N_6^M = 0)$$

$$\frac{\partial \overline{Q}_1}{\partial x} + \frac{\partial \overline{Q}_6}{\partial y} + c_2\left(\frac{\partial^2 \hat{P}_1}{\partial x^2} + 2\frac{\partial^2 \hat{P}_6}{\partial x \partial y} + \frac{\partial^2 \hat{P}_2}{\partial y^2}\right) + q = 0$$

$$\frac{\partial M_1}{\partial x} + \frac{\partial M_6}{\partial y} - Q_1 - \frac{\partial}{\partial x}(M_1^T + M_1^T) - \frac{\partial}{\partial y}(M_6^T + M_6^M) = 0$$

$$\frac{\partial M_6}{\partial x} + \frac{\partial M_2}{\partial y} - Q - \frac{\partial}{\partial y}(M_2^T + M_2^M) - \frac{\partial}{\partial x}(M_6^T + M_6^M) = 0 \tag{10}$$

where,

$M_i = \beta M_i - \gamma c_2 P_i$, $P_i = \gamma c_2 P_i + \alpha M_i$ $(i=1, 2, 6)$

$Q_i = \beta Q_i - \gamma c_1 K_i$, $\overline{Q}_i = \beta(1-\alpha)Q_i - \gamma c_1 K_i$

$(i=x, y)$,

$c_1 = 4/h^2$, $c_2 = c_1/3$, N_i, M_i, P_i, Q_i and K_i are the stress resultants.

The equlibrium equation of the classical laminate theory is obtained by setting $\alpha=1$, $\beta=0$ and $\gamma=0$. The equlibrium equation of the first-order shear deformation theory can be deduced by setting $\alpha=0$, $\beta=1$ and $\gamma=0$. The equlibrium equation of the higher-order laminate theory[8),9)] can be obtained by setting $\alpha=0$, $\beta=1$ and $\gamma=1$.

The laminate constitutive equations are relations between the stress resultants and the strains.

$$\begin{Bmatrix} N \\ M \\ P \end{Bmatrix} = \begin{bmatrix} A_{ij} & B_{ij} & E_{ij} \\ B_{ij} & D_{ij} & F_{ij} \\ E_{ij} & F_{ij} & H_{ij} \end{bmatrix} \begin{Bmatrix} \varepsilon \\ \chi \\ \chi^2 \end{Bmatrix} - \begin{Bmatrix} N^T \\ M^T \\ P^T \end{Bmatrix} - \begin{Bmatrix} N^M \\ M^M \\ P^M \end{Bmatrix}$$

$$\begin{Bmatrix} Q_x \\ Q_y \\ K_x \\ K_y \end{Bmatrix} = \begin{bmatrix} A_{55} & A_{45} & D_{55} & D_{45} \\ A_{45} & A_{44} & D_{45} & D_{44} \\ D_{55} & D_{45} & F_{55} & F_{45} \\ D_{45} & D_{44} & F_{45} & F_{44} \end{bmatrix} \begin{Bmatrix} \varepsilon_{xz}^o \\ \varepsilon_{yz}^o \\ \chi_{xz}^2 \\ \chi_{yz}^2 \end{Bmatrix} \tag{11}$$

where A_{ij}, B_{ij}, D_{ij}, etc., are the stiffnesses, defined by

$$(A_{ij}, B_{ij}, D_{ij}, E_{ij}, F_{ij}, H_{ij}) = \int_{-h/2}^{h/2} \overline{Q}_{ij}(1, z, z^2, z^3, z^4, z^6)dz \quad (i=1, 2, 6, 5, 4) \tag{12}$$

3. HYGROTHERMAL BENDING SOLUTIONS

Here the solutions of equation (10) for simply supported plates and shells are to be considered. The following simply supported boundary conditions are assumed[10)]

$$\left.\begin{matrix} u(x, 0) = u(x, b) = v = (0, y) = v(a, y) = 0 \\ N_2(x, 0) = N_2(x, b) = N_1(0, y) = N_1(a, y) = 0 \end{matrix}\right\}$$

cross-ply

$$\left.\begin{matrix} u(0, y) = u(a, y) = v(x, 0) = v(x, b) \\ N_2(0, y) = N_2(a, y) = N_1(x, 0) = N_1(x, b) = 0 \end{matrix}\right\}$$

angle-ply

$$w(x, 0)=w(x, b)=w(0, y)=w(a, y)=0$$

$$\phi_1(x, 0)=\phi_1(x, b)=\phi_2(0, y)=\phi_2(a, y)=0$$

$$P_2(x, 0)=P_2(x, b)=P_1(0, y)=P_1(a, y)=0$$

$$M_2(x, 0)=M_2(x, b)=M_1(0, y)=M_1(a, y)=0 \tag{13}$$

We assumes the following form of spatial variation of (w, ϕ_1, ϕ_2) that satisfies the boundary conditions in equation[13)]

$$w=\sum_{m, n=1}^{\infty} W_{mn} f_3(X, Y),\ \phi_1=\sum_{m, n=1}^{\infty} X_{mn} f_2(X, Y)$$

$$\phi_2=\sum_{m, n=1}^{\infty} Y_{mn} f_1(X, Y) \tag{14}$$

The variation of u, v, T_0, T_1, M_0 and M_1 is different for cross-ply and antisymmetric angle-ply laminates. For cross-ply laminates,

$$u=\sum_{m, n=1}^{\infty} U_{mn} f_2(X, Y),\ v=\sum_{m, n=1}^{\infty} V_{mn} f_1(X, Y)$$

$$T_0=\overline{T}_0^{mn} f_3(X, Y),\ T_1=\overline{T}_1^{mn} f_3(X, Y)$$

$$M_0=\overline{M}_0^{mn} f_3(X, Y),\ M_1=\overline{M}_1^{mn} f_3(X, Y) \tag{15}$$

for antisymmetric angle-ply laminates,

$$u=\sum_{m, n=1}^{\infty} U_{mn} f_1(X, Y),\ v=\sum_{m, n=1}^{\infty} V_{mn} f_2(X, Y) \tag{16}$$
$$T_0=\overline{T}_0^{mn} f_3(X, Y),\ T_1=\overline{T}_1^{mn} f_3(X, Y),$$
$$M_0=\overline{M}_0^{mn} f_3(X, Y),\ M_1=\overline{M}_1^{mn} f_3(X, Y)$$

or

$$T_0=\overline{T}_0^{mn} f_4(X, Y),\ T_1=\overline{T}_1^{mn} f_4(X, Y),$$
$$M_0=\overline{M}_0^{mn} f_4(X, Y),\ M_1=\overline{M}_1^{mn} f_4(X, Y)$$

where

$$f_1(X, Y)=\sin\alpha x\ \cos\beta y,$$
$$f_2(X, Y)=\cos\alpha x\ \sin\beta y,$$
$$f_3(X, Y)=\sin\alpha x\ \sin\beta y,$$
$$f_4(X, Y)=\cos\alpha x\ \cos\beta y \quad \text{and}$$
$$\alpha=m\pi/a,\ \beta=n\pi/b.$$

Substituting equation (14) - (16) for equation (10), and collecting the coefficients, one obtains

$$[C_{ij}]\{\triangle\}=\{F\}-\{F^T\}-\{F^M\} \tag{17}$$

matrix $[C_{ij}]$ is the coefficient matrix, $\{\triangle\}=\{U_{mn}V_{mn}W_{mn}X_{mn}Y_{mn}\}^T$, $\{F\}$ is the force vector, $\{F\}^T$ and $\{F^M\}$ are the hygrothermal force vector .

4. NUMERICAL EXAMPLES

For illustrative purposes, the hygrothermal deflection has been calculated for cross-ply and various angle-ply laminates. The Young's moduli, shear moduli, Poisson's ratio, and coefficints of hygrothermal expansion for each lamina are arbitrarily taken to be, respectively,[11)]

$$E_1=25E_2,\ G_{12}=G_{13}=0.5E_2,\ G_{23}=0.2E_2$$
$$E_2=1.0GPa,\ a/t=10(a,\ b=1m)$$
$$\alpha_1=1.0\times10^{-6}/^{\circ}C,\ \alpha_2=3.0\times10^{-6}/^{\circ}C$$
$$\nu_{12}=0.25 \tag{18}$$

Unless otherwise stated, the following nondimensional deflections and stresses have been used throughout the calculations:

$$\overline{w}=w(a/2,\ b/2)10/(\alpha_1\overline{T}_1b^2)$$
$$\overline{\sigma}_x=\sigma_x(a/2,\ b/2,\ -t/2)10/(b\alpha_1\overline{T}_1E_2)$$
$$\overline{\sigma}_y=-\sigma_y(a/2,\ b/2,\ t/2)10/(b\alpha_1\overline{T}_1E_2) \tag{19}$$

The laminated plate is composed of a finite number of layers of uniform thickness, as

shown in Fig. 2.

To validate the derived equations, the obtained thermal deflections and stresses of simply supported isotropic and cross-ply plates subjected to a uniform temperature increase are compared with these of Khdeir and Reddy[5] and Reddy[7] in Table 1-2. They are in excellent agreement. Fig. 3. consider an antisymmetric laminate having different ply angles in successive layers and shows the influence of ply angle θ_2 on thermal deflection for certain fixed value ($\pm 45°$) of θ_1. Fig. 4. shows the influence of ply angle θ on the thermal deflection for angle-ply laminates. Result are presented for plates of four and eight layers. The effect of plate thickness on the thermal deflection for square laminates having ply angle 45°/-45°/45°/-45° is illustrated in Fig. 5. For the

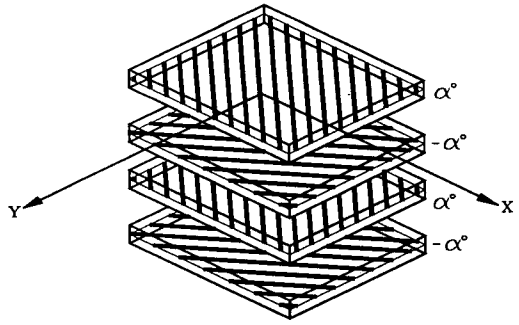

Fig. 2 Antisymmetric angle-ply laminated plate construction

Table 1 Thermal deflection $\bar{\omega}$ for isotropic and laminated plates

Angle	a/t	CLPT (ref. 5)	FSDT (ref. 5)	TSDT (ref. 5)	Present
0°	5	1.0312	1.0721	1.0711	1.0710701
	10	1.0312	1.0440	1.0439	1.0438845
0°/90°	5	1.1504	1.1504	1.1430	1.1429511
	10	1.1504	1.1504	1.1485	1.1148480
0 °/90°/0°	5	1.0312	1.0763	1.0874	1.0873640
	10	1.0312	1.0460	1.0499	1.0498593
45°/-45°/45°/-45°	5	-	-	-	0.6482121
	10	-	-	-	0.6326718

Table 2 Thermal stresses $\bar{\sigma}_x$, $\bar{\sigma}_y$ for cross-ply laminated plates

Angle	a/t	CLPT (ref. 7)		FSDT (ref. 7)		HSDT (ref. 7)		present	
		$\bar{\sigma}_x$	$\bar{\sigma}_y$	$\bar{\sigma}_x$	$\bar{\sigma}_y$	$\bar{\sigma}_x$	$\bar{\sigma}_y$	$\bar{\sigma}_x$	$\bar{\sigma}_y$
0°/90°	5	-	-0.6148	-	-0.6148	-	-0.5846	-0.5846	-0.5846
	10	-	-0.3074	-	-0.3074	-	-0.3036	-0.3036	-0.3036
0°/90°/0°	5	0.0526	-	0.4072	-	0.1154	-	0.1154	1.8775
	10	0.0263	-	0.0847	-	0.0372	-	0.0372	0.9738

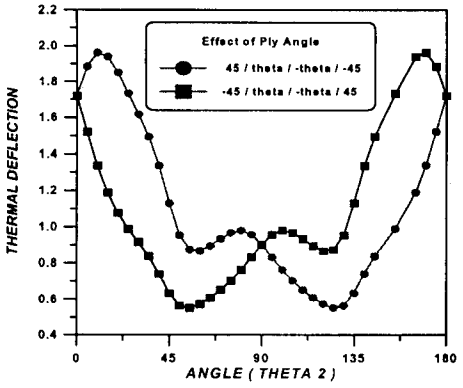

Fig. 3 Effect of ply angle on the thermal deflection

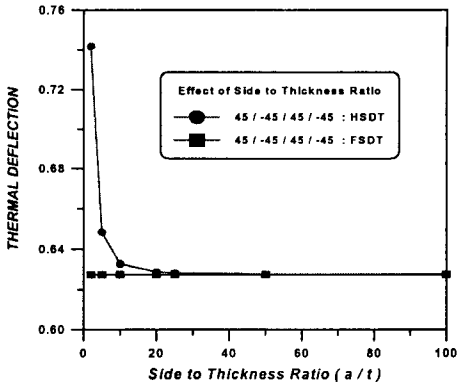

Fig. 5 Effect of side to thickness ratio on the thermal deflection

cases considered it is evident that the thermal deflection predicted by the first-order shear deformation theory is smaller than that calculated according to the higher-order shear deformation theory; the different are particularly significant for $a/t<10$. Fig. 6. shows the influence of modulus ratio E_1/E_2 upon the thermal deflection. It is observed that the thermal deflection decreases rapidly as the modulus ratio increases.

Next, the cross-ply laminated shell is composed of a finite number of layers of uniform thickness, as shown in Fig. 7.

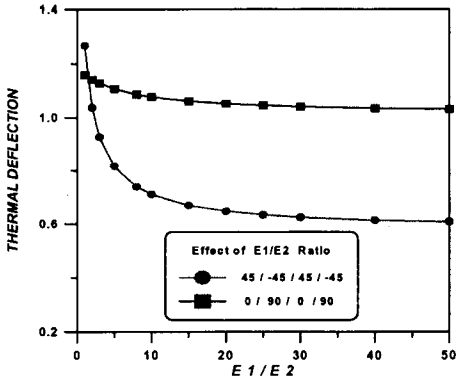

Fig. 6 Effect of elastic moduli ratio on the thermal deflection

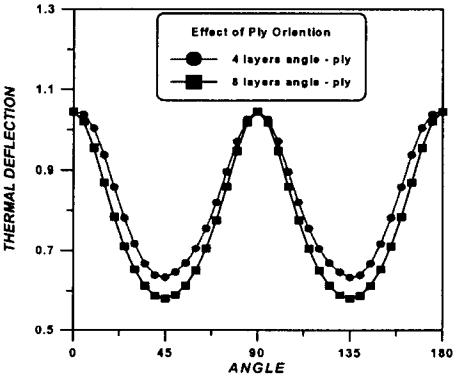

Fig. 4 Effect of ply orientation on the thermal deflection

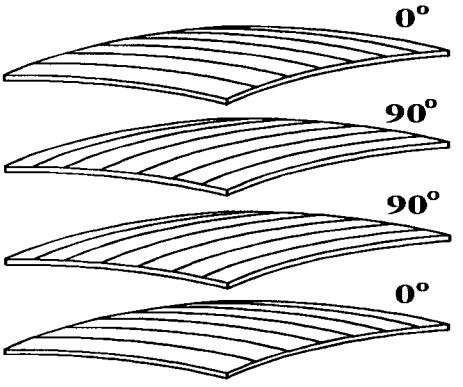

Fig. 7 Cross-ply laminated shell construction

Fig. 8. and Fig. 9. contain plots of center line (Y=b/2) deflections w and u, w, ϕ_x for plate and shell. A comparison of the center transverse deflection of the laminated plates and shells is presented in Fig. 8. Fig. 8 shows the influence of radius ratio R/a upon the thermal deflection. It is observed that the thermal deflection decreases as the radius ratio increases. Fig. 9. shows the influence of thermal coefficients upon the center line deflections u, w, ϕ_x. Fig. 10. shows the influence of thermal and hygroscopic coefficients upon the center line deflections v, w, ϕ_x. The mathematical formulations governing hygrothermal loading are analogous, generalization of the given thermoelastic solutions to thermoelastic situations is straightforward.

Fig. 11-12. shows the distribution of nondimensionalized maximum normal stressrm $\bar{\sigma}_x$by side-to-thickness ratio a/t. Fig. 11 contains two layers laminated composite plate and Fig. 12 contains the three layers plate. Fig. 11-12. shows the influence of side-to-thickness ratio a/t upon the thermal stress. It is observed that the thermal stress increases as the side-to-thickness ratio decreases. Because of higher -order shear deformation theory, the stress distribution of $a/t=10$ is cubic variation. Fig. 13. shows the difference of symmetric cross-ply and antisymmetric cross-ply. At the top of the antisymmetric cross-ply laminated plates

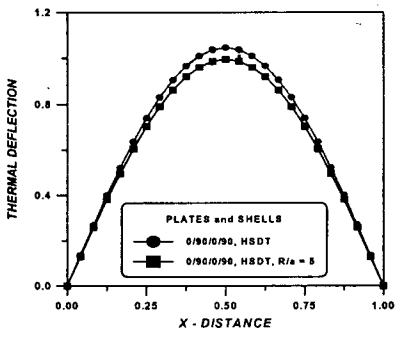

Fig. 8 Thermal deflection of laminated plates and shells

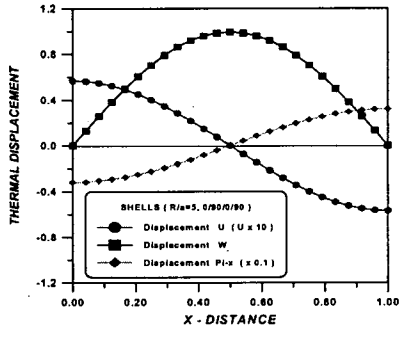

Fig. 9 Thermal deflection of cross-ply laminated shells

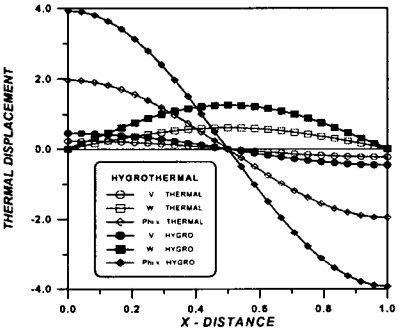

Fig. 10 Hygrothermal effect of angle-ply plates on the thermal deflection

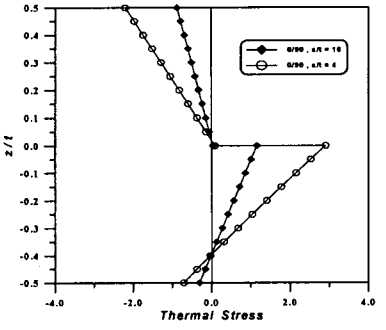

Fig. 11 Normal stress $\bar{\sigma}_x$ distribution by a/t ratio